Pramana – J. Phys. (2018) 90:23
https://doi.org/10.1007/s12043-017-1512-y

Rogue waves in the multicomponent Mel'nikov system and multicomponent Schrödinger–Boussinesq system

BAONAN SUN[1,2,3,*] and ZHAN LIAN[2,3]

[1]College of Oceanic and Atmospheric Sciences, Ocean University of China, Qingdao 266100, People's Republic of China
[2]Laboratory for Regional Oceanography and Numerical Modeling, Qingdao National Laboratory for Marine Science and Technology, Qingdao 266000, People's Republic of China
[3]Key Laboratory of Marine Science and Numerical Modeling, The First Institute of Oceanography, State Oceanic Administration, Qingdao 266061, People's Republic of China
*Corresponding author. E-mail: baonansun@126.com

MS received 21 July 2017; revised 15 September 2017; accepted 22 September 2017;
published online 10 January 2018

Abstract. By virtue of the bilinear method and the KP hierarchy reduction technique, exact explicit rational solutions of the multicomponent Mel'nikov equation and the multicomponent Schrödinger–Boussinesq equation are constructed, which contain multicomponent short waves and single-component long wave. For the multicomponent Mel'nikov equation, the fundamental rational solutions possess two different behaviours: lump and rogue wave. It is shown that the fundamental (simplest) rogue waves are line localised waves which arise from the constant background with a line profile and then disappear into the constant background again. The fundamental line rogue waves can be classified into three: bright, intermediate and dark line rogue waves. Two subclasses of non-fundamental rogue waves, i.e., multirogue waves and higher-order rogue waves are discussed. The multirogue waves describe interaction of several fundamental line rogue waves, in which interesting wave patterns appear in the intermediate time. Higher-order rogue waves exhibit dynamic behaviours that the wave structures start from lump and then retreat back to it. Moreover, by taking the parameter constraints further, general higher-order rogue wave solutions for the multicomponent Schrödinger–Boussinesq system are generated.

Keywords. Multicomponent Mel'nikov system; multicomponent Schrödinger–Boussinesq system; rogue waves; bilinear transformation method.

PACS Nos **02.30.Jr; 03.75.Lm; 04.20.Jb; 05.45.Yv**

1. Introduction

Rogue waves are unexpectedly large displacements evolving from an otherwise calm sea, and were originally observed in the oceans [1]. Recently, more and more effort was devoted to the study of such rare extreme events in areas as diverse as nonlinear optics [2,3], Bose–Einstein condensates [4], plasma physics [5], and so on [6–9]. A possible mechanism for the formation of rogue waves is associated with modulation instability [10–13]. Mathematically, fundamental (i.e., first-order) rogue wave solution, which is localised in both space and time, was first reported by Peregrine [14]. The amplitude of the first-order rogue wave reaches three times the height of the background, and then decays algebraically to the background finally. Recently, a variety of nonlinear soliton equations possessing rogue wave solutions have been verified [15–41]. Two recent articles [42,43] have provided a good review on the rogue waves from the physical view.

A variety of complex systems, such as Bose–Einstein condensates, nonlinear optical fibers, etc., usually involve more than one component [44–47]. It is of great interest to study the multicomponent nonlinear systems as the nonlinear interaction of multiple waves may result in some new physical phenomena [48–52]. Recent studies are extended to rogue waves in multicomponent systems [44,53,54]. Some new structures such as dark rogue waves have been presented numerically and analytically [53,54].

In this work, we consider the multicomponent Mel'nikov system

$$u_{tt} - u_{xy} - \left(3u^2 + u_{xx} + \sum_{\ell=1}^{M} \delta_\ell |\chi^{(\ell)}|^2\right)_{xx} = 0,$$
$$i\chi_t^{(\ell)} = u\chi^{(\ell)} + \chi_{xx}^{(\ell)}, \qquad \ell = 1, 2, 3, \ldots, M. \tag{1}$$

In eq. (1), $\chi^{(\ell)}$ represents the ℓth complex short wave envelope. u indicates the long wave amplitude (real) and the subscripts represent the partial derivatives with respect to the evolutional coordinate t and the spatial coordinates (y and x). It may be considered either as a generalisation of the Kadomtsev–Petviashvili (KP) equation with the addition of a complex scalar field or as a generalisation of the NLS equation with a real scalar field. The above system is found to be completely integrable for arbitrary nonlinearity coefficients δ_ℓ [47,55]. General dark–dark and bright–dark soliton solutions have been discussed in [47,55]. When one takes $M = 1$, this system is the one-component Mel'nikov system [56–59]. The Mel'nikov system supports boomeron-type solutions, which can be realised from an asymptotic analysis of the two-soliton solution [58]. High-order soliton solutions were also derived by Hase *et al* [60]. Besides, exponentially localised solutions [61] and rogue wave solutions [62] were also discussed.

Moreover, when taking $y = x$ in eq. (1), the multicomponent Mel'nikov system reduces to the multicomponent Schrödinger–Boussinesq equation

$$u_{tt} - u_{xx} - \left(3u^2 + u_{xx} + \sum_{\ell=1}^{M} \delta_\ell |\chi^{(\ell)}|^2\right)_{xx} = 0,$$
$$i\chi_t^{(\ell)} = u\chi^{(\ell)} + \chi_{xx}^{(\ell)}, \qquad \ell = 1, 2, 3, \ldots, M, \tag{2}$$

which is a generalisation of the Schrödinger–Boussinesq equation. The Schrödinger–Boussinesq equation is known to describe the nonlinear propagation of coupled Langmuir and dust-acoustic wave in a multicomponent dusty plasma [63]. Hase and Satsuma have obtained N-soliton solution of this system [64]. The complete integrability of this system has been studied from the view of Painlevé analysis [65]. Homoclinic and rogue wave solutions have been obtained by employing the Hirota's bilinear method [66,67].

The goal of the present paper is to derive general rational solutions including rogue waves to the multicomponent Mel'nikov system and the multicomponent Schrödinger–Boussinesq equation. The basic idea is to treat the Mel'nikov equation as a constrained KP hierarchy [68,69]. Then, rational solutions of the Mel'nikov equation are generated from τ-functions of the KP hierarchy. By taking further parameter constraints, rogue wave solutions of the multicomponent Schrödinger–Boussinesq are reduced from the corresponding rational solutions of the Mel'nikov equation.

The organisation of this paper is as follows: In §2, the main theorem, which is used to express general rational solutions of the multicomponent Mel'nikov system (1) by order-N determinant, is presented with the help of the bilinear transformation method. The explicit forms and dynamics of rational solutions are discussed in §3. The rogue wave solution of the multicomponent Schrödinger–Boussinesq equation is derived through the further reduction of the corresponding solutions of the multicomponent Mel'nikov system, and its dynamics are studied in §4. The summary is given in §5.

2. Derivation of rational solutions in the determinant form

To use the Hirota's bilinear method for deriving rational solutions of the multicomponent Mel'nikov equation, we consider a dependent variable transformation

$$\chi^{(\ell)} = \rho_\ell e^{i(k_\ell x + k_\ell^2 t)} \frac{g^{(\ell)}}{f}, \quad u = 2(\log f)_{xx}, \tag{3}$$

and the multicomponent Mel'nikov system (1) is cast into the following bilinear form:

$$(D_x^2 + 2ik^{(\ell)} D_x - iD_t) g^{(\ell)} \cdot f = 0,$$
$$(D_x^4 + D_x D_y - 3D_t^2) f \cdot f = \sum_{\ell=1}^{M} \delta_\ell \rho_\ell^2 (f^2 - g^{(\ell)} g^{(\ell)*}), \tag{4}$$

where f is a real function and $g^{(\ell)}$ is a complex function, and the operator D is the Hirota's bilinear differential operator [70] defined by

$$P(D_x, D_y, D_t) F(x, y, t, \ldots) G(x, y, t, \ldots) = P(\partial_x - \partial_{x'}, \partial_y - \partial_{y'}, \partial_t - \partial_{t'}, \ldots) \times F(x, y, t, \ldots) G(x', y', t', \ldots)|_{x'=x, y'=y, t'=t},$$

where P is a polynomial of $D_x, D_y, D_t, \ldots$. Obviously, $\chi^{(\ell)}$ and u allow for non-zero asymptotic condition $(\chi^{(\ell)}, u) \to (\rho_\ell, 0)$ as $x, y, t \to \infty$.

Theorem 1. *The multicomponent Mel'nikov system has rational solutions* (3) *with* $g^{(\ell)}$ *and* f *given by* $N \times N$ *determinants*

$$f = \tau(n)|_{n=0}, \qquad g^{(\ell)} = \tau(n^{(\ell)} + 1)|_{n=0}, \tag{5}$$

where $(n) = (n^{(1)}, n^{(2)}, \ldots, n^{(M)})$, $(n^{(\ell)} \pm 1) = (n^{(1)}, n^{(2)}, \ldots, n^{(\ell)} \pm 1, \ldots, n^{(M)})$ *and* $n = 0$ *represents* $n^{(1)} = n^{(2)} = \cdots = n^{(\ell)} = \cdots = n^{(M)} = 0$, $\tau(n) = \det_{1<i,j\le N}(m_{i,j}^{(n)})$ *and the matrix elements are defined by*

$$m_{i,j}(n) = \prod_{\ell=1}^{M}\left(-\frac{p_i - ik_\ell}{p_j^* + ik_\ell}\right)^{n^{(\ell)}} F_{i,j}\frac{1}{p_i + p_j^*}. \tag{6}$$

Here the operator

$$F_{i,j} = \sum_{k=0}^{n_i} c_{ik}\left(\partial_{p_i} + \xi_i' + \sum_{\ell=1}^{M}\frac{n^{(\ell)}}{p_i - ik_\ell}\right)^{n_i-k} \times \sum_{l=0}^{n_j} c_{jl}^*\left(\partial_{p_j^*} + \xi_i'^* + \sum_{\ell=1}^{M}\frac{n^{(\ell)}}{p_j + ik_\ell}\right)^{n_j-l}$$

and

$$\xi_i' = x - \left[12p_i^2 + \frac{1}{2}\sum_{\ell=1}^{M}\frac{\delta_\ell\rho_\ell^2}{(p_i - ik_\ell)^2}\right]y - 2ip_i t, \tag{7}$$

where p_i, c_{ik} *are arbitrary complex constants and* n_i *is an arbitrary non-negative integer.*

By a scaling of $m_{ij}(n)$, *we can normalise* $c_{i0} = 1$ *without loss of generality, and thus hereafter set* $c_{i0} = 1$. *These rational solutions can also be expressed in terms of Schür polynomials as shown in* [17,34]. *Now, we shall give a short proof for this theorem and the non-singularity of these rational solutions.*

Lemma 1. *Based on the Sato theory for the KP hierarchy* [68], *the bilinear equations in the KP hierarchy*

$$\begin{aligned}
&(D_{x_1}^2 + 2a_\ell D_{x_1} - D_{x_2})\tau(n^{(\ell)} + 1)\cdot\tau(n^{\ell}) = 0,\\
&(D_{x_1}^4 - 4D_{x_1}D_{x_3} + 3D_{x_2}^2)\tau(n^{\ell})\cdot\tau(n^{\ell}) = 0,\\
&(D_{x_1}D_{x_{-1}} - 2)\tau(n^{\ell})\cdot\tau(n^{\ell})\\
&\quad = -2\tau(n^{(\ell)} + 1)\cdot\tau(n^{(\ell)} - 1),
\end{aligned} \tag{8}$$

for $\ell = 1, 2, \ldots, M$, a_ℓ *are complex constants and* $n^{(\ell)}$ *are integers, have the Gram determinant solutions*

$$\tau(n) = \det_{1\le i,j\le N}(m_{ij}(n)), \tag{9}$$

with the matrix element $m_{ij}(n)$ *satisfying the following differential and difference relations*:

$$\begin{aligned}
\partial_{x_1} m_{ij}(n) &= \psi_i(n)\phi_j(n),\\
\partial_{x_2} m_{ij}(n) &= \psi_i(n+1)\phi_j(n) + \psi_i(n)\phi_j(n-1),\\
\partial_{x_3} m_{ij}(n) &= \psi_i(n+2)\phi_j(n) + \psi_i(n+1)\phi_j(n-1)\\
&\quad + \psi_i(n)\phi_j(n-2),\\
\partial_{x_4} m_{ij}(n) &= \psi_i(n+3)\phi_j(n) + \psi_i(n+2)\phi_j(n-1)\\
&\quad + \psi_i(n+1)\phi_j(n-2)\\
&\quad + \psi_i(n)\phi_j(n-3),\\
m_{ij}(n+1) &= m_{ij}(n+1) + \psi_i(n)\phi_j(n+1),\\
\partial_{x_v}\psi_i &= \psi_i(n+v),\\
\partial_{x_v}\phi_j &= -\phi_j(n-v) \quad (v = 1, 2, 3).
\end{aligned} \tag{10}$$

This Lemma can be proved by a similar way as the proof of the Lemma 1 of refs [17,69], and we would not prove it again. Next we use this lemma to prove Theorem 1.

Proof of Theorem 1. In order to construct rational solutions for the multicomponent Mel'nikov system, we choose functions $m_{ij}(n)$, $\psi_i(n)$ and $\phi_j(n)$ as follows:

$$\begin{aligned}
\psi_i(n) &= A_i\prod_{\ell=1}^{M}(p_i - a_\ell)^{n^{(\ell)}}\mathrm{e}^{\xi_i},\\
\phi_j(n) &= B_j\prod_{\ell=1}^{M}(-q_j - a_\ell)^{-n^{(\ell)}}\mathrm{e}^{\eta_j},\\
m_{ij}(n) &= A_iB_j\frac{1}{p_i + q_j}\mathrm{e}^{\xi+\eta}\prod_{\ell=1}^{M}\left(-\frac{p_i - a_\ell}{q_j + a_\ell}\right)^{n^{(\ell)}},
\end{aligned} \tag{11}$$

where

$$\begin{aligned}
A_i &= \sum_{k=0}^{i} c_{ik}(\partial_{p_i})^{i-k}, \qquad B_j = \sum_{l=0}^{j} d_{jl}(\partial_{q_j})^{j-l},\\
\xi_i &= \sum_{\ell=1}^{M}\frac{1}{p_i - a_\ell}r_\ell + p_i x_1 + p_i^2 x_2 + p_i^3 x_3,\\
\eta_j &= \sum_{\ell=1}^{M}\frac{1}{q_j + a_\ell}r_\ell + q_j x_1 - q_j^2 x_2 + q_j^3 x_3.
\end{aligned}$$

By taking the operator relations

$$\begin{aligned}
&\partial_{p_i}\prod_{\ell=1}^{M}(p_i - a_\ell)^{n^{(\ell)}}\mathrm{e}^{\xi_i}\\
&\quad = \prod_{\ell=1}^{M}(p_i - a_\ell)^{n^{\ell}}\mathrm{e}^{\xi_i}\left(\partial_{p_i} + \xi_i' + \sum_{\ell=1}^{M}\frac{n^{(\ell)}}{p_i - a_\ell}\right),\\
&\partial_{q_j}\prod_{\ell=1}^{M}(-q_j - a_\ell)^{n^{-(\ell)}}\mathrm{e}^{\eta_j}\\
&\quad = \prod_{\ell=1}^{M}(-q_j - a_\ell)^{-n^{\ell}}\mathrm{e}^{\eta_j}\left(\partial_{q_j} + \eta_j' - \sum_{\ell=1}^{M}\frac{n^{(\ell)}}{q_j + a_\ell}\right),
\end{aligned} \tag{12}$$

where

$$\xi_i' = -\sum_{\ell=1}^{M} \frac{r_\ell}{(p_i - a_\ell)^2} + x_1 + 2p_i x_2 + 3p_i^2 x_3,$$
$$\eta_j' = -\sum_{\ell=1}^{M} \frac{r_\ell}{(q_i + a_\ell)^2} + x_1 - 2q_j x_2 + 3q_j^2 x_3, \quad (13)$$

functions $m_{ij}(n)$ are rewritten simply as

$$m_{i,j}(n) = \prod_{\ell=1}^{M} \left(-\frac{p_i - a_\ell}{q_j + a_\ell}\right)^{n^{(\ell)}} \mathrm{e}^{\xi_i + \eta_j} F_{i,j} \frac{1}{p_i + q_j}, \quad (14)$$

where the operator

$$F_{i,j} = \sum_{k=0}^{n_i} c_{ik} \left(\partial_{p_i} + \xi_i' + \sum_{\ell=1}^{M} \frac{n^{(\ell)}}{p_i - a_\ell}\right)^{n_i - k} \times \sum_{l=0}^{n_j} d_{jl} \left(\partial_{q_j} + \xi_j' - \sum_{\ell=1}^{M} \frac{n^{(\ell)}}{q_j + a_\ell}\right)^{n_j - l}. \quad (15a)$$

Here p_i, q_j, c_{ik}, d_{jl} are arbitrary complex constants, and i, j, n_i, N are arbitrary positive integers.

Further, taking the parameter constraints

$$q_j = p_j^*, \quad d_{jl} = c_{jl}^*, \quad a_\ell = ik_\ell \quad (16)$$

and assuming x_1, x_3 are real, x_2 is pure imaginary, we have

$$\eta' = \xi'^*, \quad m_{ij}^*(n) = m_{ji}(-n), \quad \tau(n)^* = \tau(-n). \quad (17)$$

Take

$$f = \tau(n)|_{n^{(1)}=n^{(2)}\cdots=n^{(\ell)}=\cdots=n^{(M)}=0},$$
$$g^{(\ell)} = \tau(n) + 1|_{n^{(1)}=n^{(2)}\cdots=n^{(\ell)}=\cdots=n^{(M)}=0}, \quad (18)$$
$$g^{(\ell)*} = \tau(n) - 1|_{n^{(1)}=n^{(2)}\cdots=n^{(\ell)}=\cdots=n^{(M)}=0},$$

then bilinear equations become

$$(D_{x_1}^2 + 2a_\ell D_{x_1} - D_{x_2}) g^{(\ell)} \cdot f = 0,$$
$$(D_{x_1}^4 - 4D_{x_1} D_{x_3} + 3D_{x_2}^2) f \cdot f = 0,$$
$$(D_{x_1} D_{x_{-1}} - 2) f \cdot f = -2g^{(\ell)} g^{(\ell)*}, \quad (19)$$

for $\ell = 1, 2, \ldots, M$. Applying the change of independent variables

$$x_1 = x, \quad x_2 = -it, \quad x_3 = -4y, \quad r_\ell = \frac{\delta_\ell \rho_\ell^2 y}{2},$$

the bilinear equation (eq. (19)) is transformed to the bilinear eq. (4). Under the gauge transformation (3), rational solutions to the multicomponent Mel'nikov system (1) given in Theorem 1 are derived from the rational solutions of eq. (8). Hence, Theorem 1 has been proved. □

Next, we concentrate on commenting that these obtained rational solutions are non-singular, that is, proving $f \neq 0$. Note that $f = \tau(0)$ is given by the determinant

$$f = \det_{1 \le i,j \le N}(m_{i,j}(0)). \quad (20)$$

Indeed, for any non-zero column vector $\mu = (\mu_1, \mu_2, \ldots, \mu_N)^T$ and $\bar{\mu}$ being its complex transpose, we have

$$\begin{aligned}
\bar{\mu} f \mu &= \sum_{i,j=1}^{N} \bar{\mu}_i m_{i,j}(0) \mu_j \\
&= \sum_{i,j=1}^{N} \bar{\mu}_i \mu_j A_i B_j \frac{1}{p_i + q_j} \mathrm{e}^{\xi_i + \eta_j}|_{q_j = p_j^*} \\
&= \sum_{i,j=1}^{N} \bar{\mu}_i \mu_j A_i B_j \int_{-\infty}^{x} \mathrm{e}^{\xi_i + \eta_j} \mathrm{d}x|_{q_j = p_j^*} \\
&= \int_{-\infty}^{x} \left(\sum_{i,j=1}^{N} \bar{\mu}_i \mu_j A_i B_j \mathrm{e}^{\xi_i + \eta_j}|_{q_j = p_j^*}\right) \mathrm{d}x \\
&= \int_{-\infty}^{x} \left|\sum_{i=1}^{N} \bar{\mu}_i A_i \mathrm{e}^{\xi_i}\right|^2 \mathrm{d}x > 0. \quad (21)
\end{aligned}$$

Thus we have proved that f is positive definite. Therefore, rational solutions $\chi^{(\ell)}$, u defined in Theorem 1 are non-singular.

3. Rational solutions to multicomponent Mel'nikov system

In this section, we proceed to demonstrate typical dynamics of these rational solutions to the multicomponent Mel'nikov system in detail.

3.1 *Fundamental rational solutions*

The simplest rational solution, namely, 1-rational solution of first-order, is given by taking $N = 1$ and $n_1 = 1$. The functions f and g_s of the solutions are expressed explicitly by the following formulae:

$$f = \sum_{k=0}^{1} c_{1k} (\partial_{p_1} + \xi_1')^{1-k} \times \sum_{l=0}^{1} c_{1l}^* (\partial_{p_1^*} + \xi_{1*}')^{1-l} \frac{1}{p_1 + p_1^*}$$

$$= (\partial_{p_1} + \xi_1' + c_{11}) \times (\partial_{p_1^*} + \xi_1'^* + c_{11}^*) \frac{1}{p_1 + p_1^*}$$
$$= \frac{1}{p_1 + p_1^*} \left[\left(\xi_1' - \frac{1}{p_1 + p_1^*} + c_{11} \right) \times \left(\xi_1'^* - \frac{1}{p_1 + p_1^*} + c_{11}^* \right) + \frac{1}{(p_1 + p_1^*)^2} \right], \quad (22)$$

$$g^{(\ell)} = \left(-\frac{p_1 - ik_\ell}{p_1^* + ik_\ell} \right) \sum_{k=0}^{1} c_{1k} \left(\partial_{p_1} + \xi_1' + \frac{1}{p_1 - ik_\ell} \right)^{1-k} \times \sum_{l=0}^{1} c_{1l}^* \left(\partial_{p_1^*} + \xi_1'^* - \frac{1}{p_1^* + ik_\ell} \right)^{1-l} \frac{1}{p_1 + p_1^*}$$
$$= \left(-\frac{p_1 - ik_\ell}{p_1^* + ik_\ell} \right) \left(\partial_{p_1} + \xi_1' + c_{11} + \frac{1}{p_1 - ik_\ell} \right) \times \left(\partial_{p_1^*} + \xi_1'^* + c_{11}^* - \frac{1}{p_1^* + ik_\ell} \right) \frac{1}{p_1 + p_1^*}$$
$$= \frac{1}{p_1 + p_1^*} \left(-\frac{p_1 - ik_\ell}{p_1^* + ik_\ell} \right) \times \left[\left(\xi_1' - \frac{1}{p_1 + p_1^*} + c_{11} + \frac{1}{p_1 - ik_\ell} \right) \times \left(\xi_1'^* - \frac{1}{p_1 + p_1^*} + c_{11}^* - \frac{1}{p_1^* + ik_\ell} \right) + \frac{1}{(p_1 + p_1^*)^2} \right], \quad (23)$$

with

$$\xi_1' = x - \left[12p_1^2 + \frac{1}{2} \sum_{\ell=1}^{M} \frac{\delta_\ell \rho_\ell^2}{(p_1 - ik_\ell)^2} \right] y - 2ip_1 t,$$

where p_1, c_{11} are arbitrary complex constants and k_ℓ are real constants.

Without loss of generality, we set $p_1 = p_{1R} + i\, p_{1I}$, $c_{11} = c_{1R} + i\, c_{1I}$ and then rewrite the above functions f and $g^{(\ell)}$ as

$$f = \theta\, \theta^* + \theta_0,$$
$$g^{(\ell)} = \frac{1}{2p_{1R}} \frac{p_{1R} + i(p_{1I} - k_\ell)}{p_{1R} - i(p_{1I} - k_\ell)} \times [(\theta + e_{\ell 1} + ie_{\ell 2})\, (\theta^* - e_{\ell 1} + ie_{\ell 2}) + \theta_0], \quad (24)$$

where

$$\theta = l_1 + il_2, \quad \theta_0 = \frac{1}{4p_{1R}^2}$$
$$l_1 = x + b_1 y + c_1 t + d_1, \quad l_2 = b_2 y + c_2 t + d_2,$$
$$b_1 = -12p_{1R}^2 - \frac{1}{2} \sum_{\ell=1}^{M} \delta_\ell \rho_\ell^2 (e_{\ell 1}^2 - e_{\ell 2}^2),$$
$$c_1 = 2p_{1I}, \quad d_1 = -\frac{1}{2p_{1R}} + c_{1R},$$
$$b_2 = -24p_{1R}p_{1I} + \sum_{\ell=1}^{M} \delta_\ell \rho_\ell^2 e_{\ell 1} e_{\ell 2},$$
$$c_2 = -2p_{1R}, \quad d_2 = c_{1I},$$
$$e_{\ell 1} = \frac{p_{1R}}{p_{1R}^2 + (p_{1I} - k_\ell)^2},$$
$$e_{\ell 2} = \frac{p_{1I} - k_\ell}{p_{1R}^2 + (p_{1I} - k_\ell)^2}. \quad (25)$$

Then, the final expressions of the fundamental semi-rational solutions are given explicitly by the following formulae:

$$\chi^{(\ell)} = \rho_\ell e^{i(k_\ell x + k_\ell^2 t)} \left[1 - \frac{2i(e_{\ell 1} l_2 - e_{\ell 2} l_1) + e_{\ell 1}^2 + e_{\ell 2}^2}{l_1^2 + l_2^2 + \theta_0} \right],$$
$$u = 4 \frac{l_2^2 - l_1^2 + \theta_0}{(l_1^2 + l_2^2 + \theta_0)^2}. \quad (26)$$

As solutions of most of the $(2 + 1)$-dimensional nonlinear systems [30,34,35,37,71], these rational solutions also possess two different dynamical behaviours:

(1) Lump solutions. When $b_2 \neq 0$, one can see that $\chi^{(\ell)}$ and u are constant along the trajectory $[x(t), y(t)]$ where

$$x + b_1 y + c_1 t + 0, \quad b_2 y + c_2 t = 0, \quad (27)$$

and $(\chi^{(\ell)}, u) \to (\rho^{(\ell)}, 0)$ as $(x, y) \to (\infty, \infty)$ at arbitrarily given time. So, solutions $\chi^{(\ell)}$ and u are lumps, which cannot disappear along time evolution but propagate with a significant amplitude on the constant background.

In general, patterns of lump solutions do not change at different time on (x, y)-plane. Hence, we can discuss the patterns of lumps at $t = 0$ without loss of generality. In this case, we proceed to calculate all the possible critical points of $|\chi^{(\ell)}|^2$ at $t = 0$. By a simple calculation, there are five possible critical points, i.e.,

$$A_1 = (x_1, y_1) = \left(\frac{b_1}{b_2} d_2 - d_1, -\frac{d_2}{b_2} \right), \quad (28)$$
$$A_2 = (x_2^{(\ell)}, y_2^{(\ell)}) = \left(-\frac{e_{\ell 2}}{e_{\ell 1}} (\lambda_{\ell 1} + d_2) - \frac{b_1}{b_2} \lambda_{\ell 1} - d_1, \frac{\lambda_{\ell 1}}{b_2} \right), \quad (29)$$
$$A_3 = (x_3^{(\ell)}, y_3^{(\ell)}) = \left(-\frac{e_{\ell 2}}{e_{\ell 1}} (\lambda_{\ell 1}' + d_2) - \frac{b_1}{b_2} \lambda_{\ell 1}' - d_1, \frac{\lambda_{\ell 1}'}{b_2} \right), \quad (30)$$

$$A_4 = (x_4^{(\ell)}, y_4^{(\ell)}) = \left(\frac{e_{\ell 1}}{e_{\ell 2}}(\lambda_{\ell 2} + d_2) - \frac{b_1}{b_2}\lambda_{\ell 2} - d_1, \frac{\lambda_{\ell 2}}{b_2}\right), \quad (31)$$

$$A_5 = (x_5^{(\ell)}, y_5^{(\ell)}) = \left(\frac{e_{\ell 1}}{e_{\ell 2}}(\lambda'_{\ell 2} + d_2) - \frac{b_1}{b_2}\lambda'_{\ell 2} - d_1, \frac{\lambda'_{\ell 2}}{b_2}\right), \quad (32)$$

where

$$\lambda_{\ell 1} = -c_{1I} + \frac{\sqrt{\gamma_{\ell 1}}}{2\gamma_{\ell 0}},$$
$$\lambda'_{\ell 1} = -c_{1I} - \frac{\sqrt{\gamma_{\ell 1}}}{2\gamma_{\ell 0}},$$
$$\lambda_{\ell 2} = -c_{1I} + \frac{\sqrt{-(p_{1I} - k_\ell)^2\gamma_{\ell 2}}}{2p_{1R}\gamma_{\ell 0}},$$
$$\lambda'_{\ell 2} = -c_{1I} - \frac{\sqrt{-(p_{1I} - k_\ell)^2\gamma_{\ell 2}}}{2p_{1R}\gamma_{\ell 0}},$$
$$\gamma_{\ell 0} = (p_{1I} - k_\ell)^2 + p_{1R}^2,$$
$$\gamma_{\ell 1} = 3(p_{1I} - k_\ell)^2 - p_{1R}^2,$$
$$\gamma_{\ell 2} = (p_{1I} - k_\ell)^2 - 3p_{1R}^2,$$

which are solved by

$$\frac{\partial|\chi^{(\ell)}|^2(x, y, 0)}{\partial x} = \frac{\partial|\chi^{(\ell)}|^2(x, y, 0)}{\partial y} = 0. \quad (33)$$

The second-order derivative of $|\chi^{(\ell)}|^2$ are: $H_1 = \partial^2|\chi^{(\ell)}|^2/\partial x^2$, $H_2 = \partial^2|\chi^{(\ell)}|^2/\partial y^2$, $H_3 = \partial^2|\chi^{(\ell)}|^2/\partial x\partial y$ and $H = H_1H_2 - H_3^2$. A tedious calculation infers

$$H(x_1, y_1) = \frac{189p_{1R}^4\gamma_{\ell 3}}{\gamma_{\ell 0}^2},$$
$$H_1(x_1, y_1) = \frac{4096b_2^2p_{1R}^8\gamma_{\ell 1}\gamma_{\ell 2}}{\gamma_{\ell 0}^4}, \quad (34)$$
$$H(x_2^{(\ell)}, y_2^{(\ell)}) = -\frac{12p_{1R}^4\gamma_{\ell 0}}{(p_{1I} - k_\ell)^4},$$
$$H_1(x_2^{(\ell)}, y_2^{(\ell)}) = \frac{32b_2^2p_{1R}^8\gamma_{\ell 0}^2\gamma_{\ell 1}}{(p_{1I} - k_\ell)^{10}}, \quad (35)$$
$$H(x_3^{(\ell)}, y_3^{(\ell)}) = -\frac{12p_{1R}^4\gamma_{\ell 0}}{(p_{1I} - k_\ell)^4},$$
$$H_1(x_3^{(\ell)}, y_3^{(\ell)}) = \frac{32b_2^2p_{1R}^8\gamma_{\ell 0}^2\gamma_{\ell 1}}{(p_{1I} - k_\ell)^{10}}, \quad (36)$$
$$H(x_4^{(\ell)}, y_4^{(\ell)}) = 6\gamma_{\ell 0},$$
$$H_1(x_4^{(\ell)}, y_4^{(\ell)}) = \frac{16b_2^2\gamma_{\ell 0}^2\gamma_{\ell 1}}{p_{1R}^2}, \quad (37)$$
$$H(x_5^{(\ell)}, y_5^{(\ell)}) = 6\gamma_{\ell 0},$$
$$H_1(x_5^{(\ell)}, y_5^{(\ell)}) = \frac{16b_2^2\gamma_{\ell 0}^2\gamma_{\ell 1}}{p_{1R}^2}, \quad (38)$$

where $\gamma_{\ell 3} = (p_{1I} - k_\ell)^2 - p_{1R}^2$.

According to A_i $(1 \le i \le 5)$, H_1 and H, the lump solutions $\chi^{(\ell)}$ in eq. (26) can be classified into three patterns.

(a) Bright lump. When $0 \le (p_{1I} - k_\ell)^2 < \frac{1}{3}p_{1R}^2$, $|\chi^{(\ell)}|$ has one local maximum (point A_1) and two local minimum points (point A_4 and A_5).
(b) Bimodel lump. When $\frac{1}{3}p_{1R}^2 \le (p_{1I} - k_\ell)^2 < 3p_{1R}^2$, $|\chi^{(\ell)}|$ has two local maximum points (points A_2 and A_3) and two local minimum points (points A_4 and A_5).
(c) Dark lump. When $(p_{1I} - k_\ell)^2 \ge 3p_{1R}^2$, $|\chi^{(\ell)}|$ has two local maximum points (points A_2 and A_3) and one local minimum point (point A_1).

The one-lump profile for the short-wave components are demonstrated in figure 1 with $M = 3$. Three components represent three different patterns of lump solution in the above classification respectively. Note that the classification of the one-lump solutions is also suitable for higher-order lump solutions.

(2) Rogue wave solution. As a special case of the rational solutions, rogue wave solutions can be obtained by taking $b_2 = 0$, that is,

$$-24p_{1R}p_{1I} + \sum_{\ell=1}^{M}\frac{k_\ell\rho_\ell^2p_{1R}(p_{1I} - k_\ell)}{[p_{1R}^2 + (p_{1I} - k_\ell)^2]^2} = 0. \quad (39)$$

Then, rational solution (26) describes a line rogue wave. It arises from the constant background with a line profile

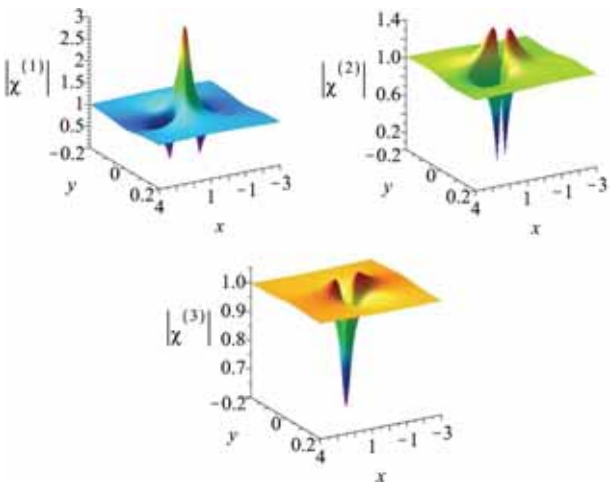

Figure 1. One-lump for the multicomponent Mel'nikov system at $t = 0$ with different parameters $(\rho_1, \rho_2, \rho_3) = (1, 1, 1)$, $(k_1, k_2, k_3) = (1, 0, 3)$, $p_1 = 1 + i$, $(\delta_1, \delta_2, \delta_3) = (1, -1, 1)$.

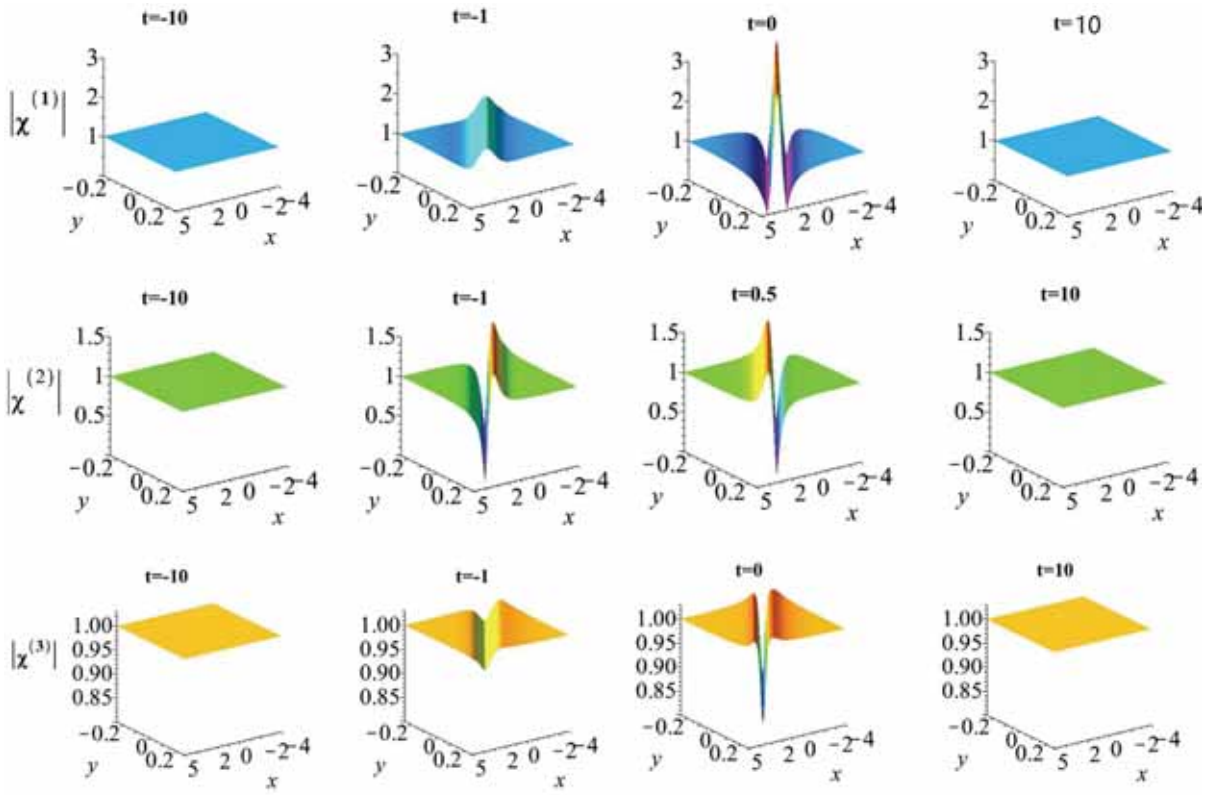

Figure 2. One-rogue wave for the multicomponent Mel'nikov system with parameters $M = 3$, $(\rho_1, \rho_2, \rho_3) = (1, 1, 1)$, $(k_1, k_2, k_3) = (1, 0, 3)$, $p_1 = 1$, $(\delta_1, \delta_2, \delta_3) = (1, 0, 0)$.

at early stage, then reaches a peak (or valley) at the intermediate time, and finally retreats back to the same background. That fact shows that the large amplitude of the line rogue wave only exists for a short period of time, which is different from a moving line-soliton on (x, y)-plane for two-dimensional integrable equations. The validity of the evolution of the line rogue wave is demonstrated in figure 2.

Based on the analysis of critical lines for rational solutions (26) under parameter constraint conditions (39), rogue wave solutions can be classified into three types:

(i) The bright line rogue wave. When $0 \leq (p_{1I} - k_\ell)^2 \leq \frac{1}{3}p_{1R}^2$, $|\chi^{(\ell)}|$ has one local maximum amplitude line and two local minimum amplitude lines.
(ii) The intermediate state line rogue wave. When $\frac{1}{3}p_{1R}^2 < (p_{1I} - k_\ell)^2 \leq 3p_{1R}^2$, $|\chi^{(\ell)}|$ has one local maximum amplitude line and one local minimum amplitude line.
(iii) The dark line rogue wave. When $(p_{1I} - k_\ell)^2 \geq 3p_{1R}^2$, $|\chi^{(\ell)}|$ has two local maximum amplitude lines and one local minimum amplitude line.

Note that fundamental rogue waves for the one-component Mel'nikov system have been discussed in ref. [72]. It has been verified that there are only bright line rogue waves in the one-component Mel'nikov system. That fact indicates that multicomponent Mel'nikov system possesses much more physical phenomena. Similar results have also been reported in the multicomponent NLS equations [44,53,54]. Compared to the one-component NLS equation, there are more different types of rogue waves in the multicomponent NLS equation, including bright–dark rogue waves and four-petaled rogue waves, while there are only bright rogue waves in the former. Typical profiles of these three types of line rogue waves are given in figure 2 for $M = 3$. Three components represent different types of fundamental rogue wave solution in the above classification.

Non-fundamental rational solutions can be obtained by taking $N > 1$, or $n_i > 1$, or both in eq. (5). These rational solutions contain multirogue waves, higher-order rogue waves and non-fundamental lumps. Below, we mainly consider two subclasses of non-fundamental rational solutions.

3.2 *Multirational solutions*

One subclass of non-fundamental rogue waves is the multirational solutions, which can be obtained by taking $N > 1, n_1 = n_2 = \cdots = n_N = 1$ in rational

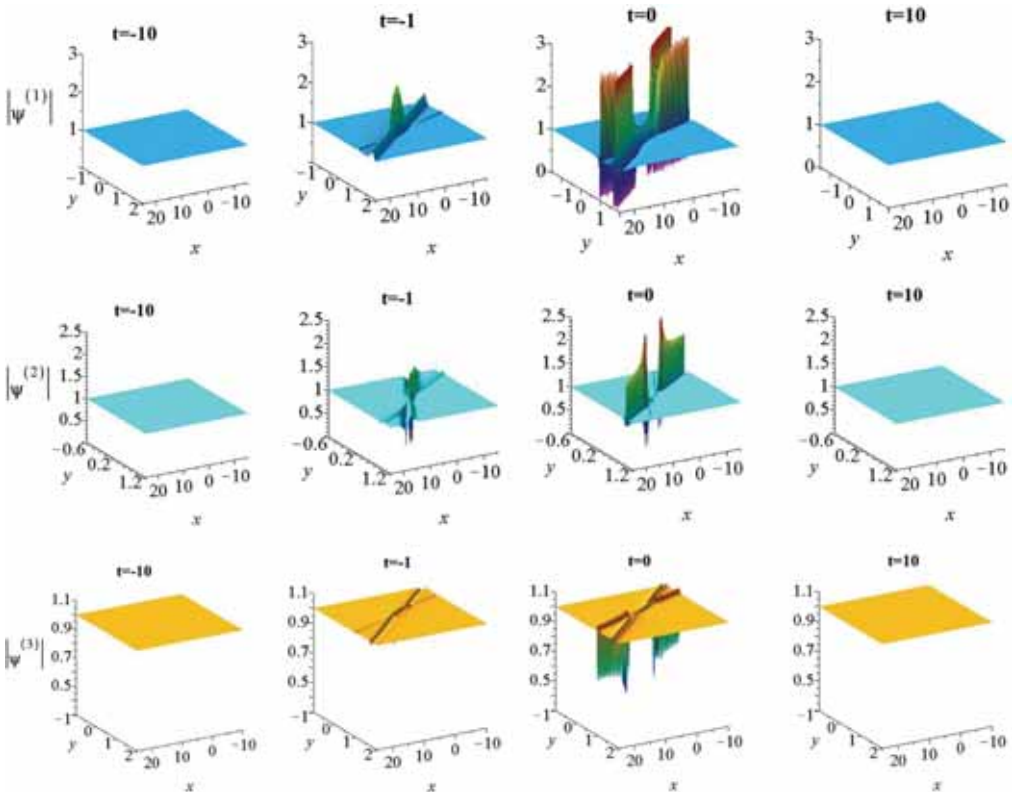

Figure 3. Two-rogue wave for the multicomponent Mel'nikov system with parameters $M = 3$, $(\rho_1, \rho_2, \rho_3) = (1, 1, 1)$, $(k_1, k_2, k_3) = (1, 0, 3)$, $p_1 = 1$, $p_2 = \frac{2}{3}$, $(\delta_1, \delta_2, \delta_3) = (1, 0, 0)$.

solutions (5). These solutions describe the interaction of N individual fundamental rational solutions, including lumps and rogue waves, which depend on whether or not the parameters meet the conditions

$$\{\mathrm{Im}(f(p_i)) = 0 | i = 1, 2, \ldots, N\}, \tag{40}$$

where Im represents the imaginary part of the functions and $f(p_i)$ is given by

$$f(p_i) = 12p_i^2 + \frac{1}{2}\sum_{\ell=1}^{M} \frac{\delta_\ell \rho_\ell^2}{(p_i - ik_\ell)^2}. \tag{41}$$

When parameters meet conditions (40), the corresponding rational solutions are multirogue waves. If not, they are multilumps, or mixed solutions consisting of rogue waves and lumps.

For example, when one takes $N = 2, n_1 = n_2 = 1$, the functions f and $g^{(\ell)}$ are

$$f = \begin{vmatrix} m_{11}^{(0)} & m_{12}^{(0)} \\ m_{21}^{(0)} & m_{22}^{(0)} \end{vmatrix}, \quad g^{(\ell)} = \begin{vmatrix} m_{11}^{(1)} & m_{12}^{(1)} \\ m_{21}^{(1)} & m_{22}^{(1)} \end{vmatrix}. \tag{42}$$

Here

$$m_{ij}^{(0)} = \frac{1}{p_i + p_j^*}\left[\zeta_i\zeta_j + \frac{1}{(p_i + p_j^*)^2}\right],$$

$$m_{ij}^{(1)} = \frac{1}{p_i + p_j^*}\left[\left(\zeta_i + \frac{1}{p_i}\right)\left(\zeta_j - \frac{1}{p_j^*}\right) + \frac{1}{(p_i + p_j^*)^2}\right],$$

and

$$\zeta_i = \xi_i' - \frac{1}{p_i + p_j^*} + c_{i1}, \quad \zeta_j^* = \xi_j'^* - \frac{1}{p_i + p_j^*} + c_{j1}^*,$$

ξ_i' is given by (7) and p_1, p_2, c_{11} and c_{21} are arbitrary complex parameters. In this case, the corresponding solutions possess three different behaviours:

(1) Multirogue waves. When $f(p_1) = f(p_2) = 0$, the corresponding rational solutions are two-rogue waves, which are demonstrated in figure 3. Here, any patterns of one-rogue wave could coexist with any patterns of one-rogue wave. Thus, there are six patterns of two-rogue wave solutions, namely, bright–bright, bright–dark, bright–intermediate, dark–dark, dark–intermediate, intermediate–intermediate rogue waves.

Table 1. The classification of two-rogue wave solution.

Region	Status
$0 < (p_{jI} - k_j)^2 \leq \frac{1}{3}p_{jR}^2 \quad (j = 1, 2)$	Bright–bright
$\frac{1}{3}p_{jR}^2 < (p_{jI} - k_j)^2 \leq 3p_{jR}^2 \quad (j = 1, 2)$	Intermediate–intermediate
$(p_{jI} - k_j)^2 > 3p_{jR}^2 \quad (j = 1, 2)$	Dark–dark
$0 < (p_{1I} - k_1)^2 \leq \frac{1}{3}p_{1R}^2, (p_{2I} - k_2)^2 > 3p_{2R}^2$	Bright–dark
$0 < (p_{1I} - k_1)^2 \leq \frac{1}{3}p_{1R}^2, \frac{1}{3}p_{2R}^2 < (p_{2I} - k_2)^2 \leq 3p_{2R}^2$	Bright–intermediate
$(p_{1I} - k_1)^2 > 3p_{1R}^2, \frac{1}{3}p_{2R}^2 < (p_{2I} - k_2)^2 \leq 3p_{2R}^2$	Dark–intermediate

The classification for patterns of the two-rogue wave solution is summarised in table 1. Here we only demonstrate three types in figure 3, i.e., bright–bright, dark–dark, intermediate–intermediate rogue waves.

As seen in figure 3, the line rogue wave of every short-wave component $\chi^{(\ell)}$ starts from the constant background in the entire (x, y)-plane as $t << 0$. In the intermediate times, all these short-wave components undergo nearly the same process in which two line rogue waves interact with each other: the regions of their intersection acquire higher/lower amplitudes first (see the panel at $t = -1$), the wave patterns form into two curvy wave fronts which are completely separated (see the $t = 0$ panel), and then these waves possess higher/lower amplitudes again in the regions of their intersection. At larger times, these solutions go back to the constant background (see the panel at $t = 5$).

(2) Multilumps. When $f(p_1) \neq 0$, $f(p_2) \neq 0$, the corresponding rational solutions are lumps. As discussed in ref. [73], these two-lump solutions also are classified into six patterns, namely, bright–bright, bright–dark, bright–intermediate, dark–dark, dark–intermediate, intermediate–intermediate lumps.

(3) Mixed solution. When $f(p_1) = 0$, $f(p_2) \neq 0$, or $f(p_1) \neq 0$, $f(p_2) = 0$, the corresponding solutions are mixed solutions composed of one lump and one line rogue wave. Typical dynamics of this kind of mixed solutions have been discussed in ref. [30].

3.3 *Higher-order rational solutions*

Another subclass of non-fundamental rational solutions is the higher-order rational solutions, which are obtained by taking $N = 1, n_1 > 1$ in rational solutions (5). In this situation, these rational solutions are classified into two types: higher-order lumps and rogue waves. If the parameters satisfy the following relations:

$$\left\{\mathrm{Im}\frac{\partial^k f(p_1)}{\partial p_1^k}\right\} = 0, \quad k = 0, 1, 2, \ldots, n_1 - 1, \tag{43}$$

the imaginary part of the coefficient of y will be zero. In this case, the corresponding rational solutions are higher-order rogue waves. If not, they are higher-order lumps.

To demonstrate this subclass of higher-order rational solutions, we consider the case of $N = 1, n_1 = 2$ in eq. (5). In this situation, functions f and g are given by

$$\begin{aligned} f &= [(\partial_{p_1} + \xi_1')^2 + c_{12}][(\partial_{p_1^*} + \xi_1'^*)^2 + c_{12}^*]\frac{1}{p_1 + p_1^*}, \\ g &= [(\partial_{p_1} + \xi_1' + 1)^2 + c_{12}][(\partial_{p_1^*} + \xi_1'^* - 1)^2 \\ &\quad + c_{12}^*]\frac{1}{p_1 + p_1^*}. \end{aligned} \tag{44}$$

Here ξ_1' is defined in Theorem 1, p_1 and c_{12} are two free complex parameters. Note that the changing of c_{11} in Theorem 1 leads to shift $|\chi^{(\ell)}|$ and $|u|$ in (x, y, t) coordinates, and thus setting $c_{11} = 0$ without loss of generality. For the general choice of the parameters, this solution represents second-order lump. When these parameters meet the constraint conditions (43) with $n_1 = 2$, this rational solution reduces to second-order rogue wave solutions.

In figure 4, the second-order rogue waves for multicomponent Mel'nikov system which still contains three short-wave components are demonstrated. Comparing to the two-rogue waves shown in figure 3, these higher-order rogue waves possess a new phenomenon: these higher-order rogue waves feature localised lumps instead of uniformly approaching the constant background as $t \to \pm\infty$. As seen from figure 4, these solutions for three short waves are localised lumps sitting on the constant backgrounds when $|t| \gg 0$ (see the panels at $t = \pm 5$). When $t \to 0$, these lumps disappear gradually and three parabola-shaped rogue waves rise from their backgrounds (see the panels at $t = -1, 0$). In addition, the classification of patterns of second-order rogue waves are summarised in table 2. The density and the three-dimensional plot of three different patterns of rogue waves are given in figure 5.

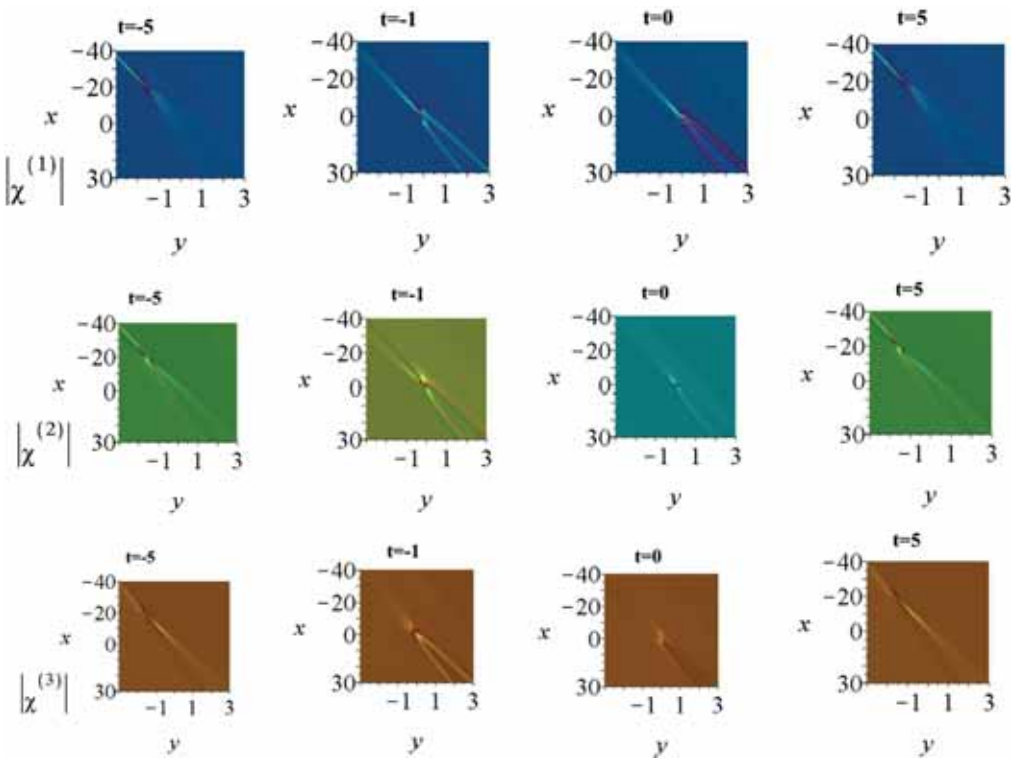

Figure 4. Second-order rogue wave for the multicomponent Mel'nikov system with parameters $M = 3$, $(\rho_1, \rho_2, \rho_3) = (1, 1, 1)$, $(k_1, k_2, k_3) = (1, 0, 3)$, $p_1 = 1$, $(\delta_1, \delta_2, \delta_3) = (1, 0, 0)$.

4. Rogue waves of the multicomponent Schrödinger–Boussinesq equation

As discussed in ref. [62], solutions of the Schrödinger–Boussinesq equation can be obtained by taking further reduction of solutions of the Mel'nikov equation. Rogue wave solutions of the multicomponent Schrödinger–Boussinesq equation can also be derived from one of the multicomponent Mel'nikov equation. Indeed, when one takes parameter constraints in eq. (5)

$$\frac{\partial \chi^{(\ell)}}{\partial_y} = \frac{\partial \chi^{(\ell)}}{\partial_x}, \quad \frac{\partial u}{\partial_y} = \frac{\partial u}{\partial_x}, \tag{45}$$

the rogue wave solutions of the multicomponent Schrödinger–Boussinesq equation can be summarised in the following theorem:

Theorem 2. *The multicomponent Schrödinger–Boussinesq equation has rational solutions*

$$\chi^{(\ell)} = \rho_\ell e^{i(k_\ell x + k_\ell^2 t)} \frac{g^{(\ell)}}{f}, \quad u = 2(\log f)_{xx}, \tag{46}$$

where ρ_ℓ and k_ℓ are real constants, and $g^{(\ell)}$ and f are defined in eq. (5) with parameters satisfying the constraints

$$\left\{ \frac{\mathrm{d}^k}{\mathrm{d}p_i^k}(f(p_i) - 1) = 0 | i = 1, 2, \ldots, N; \right.$$
$$\left. k = 0, 1, 2, \ldots, n_i \right\}. \tag{47}$$

The fundamental rogue wave solutions can be obtained by taking $N = 1, n_i = 1, k = 0$ in Theorem 2, that is

$$f(p_1) - 1 = 0.$$

As fundamental lumps or fundamental line rogue waves of the multicomponent Mel'nikov equation, fundamental rogue wave of the multicomponent Schrödinger–Boussinesq equation also possess three states: bright, four-petaled and dark rogue waves. Based on the analysis of critical points for fundamental rogue waves, the classification of the fundamental rogue waves are summarised in table 3. Three different types of rogue wave structures are demonstrated for every short-wave components in figure 6.

As in the multicomponent Mel'nikov systems, there are two subclasses of non-fundamental rogue waves in the multicomponent Schrödinger–Boussinesq equation: multi- and higher-order rogue wave. Specifically, by restricting parameters

$$\{f(p_i) - 1 = 0 | i = 1, 2, \ldots, N\},$$

Table 2. The classification of second-order rational solutions.

Discriminant	Region	Type
$\mathrm{Im}\{\frac{\partial^k f(p_1)}{\partial p_1^k}\} = 0, k = 0, 1$	$0 < (p_{1I} - k_\ell)^2 \leq \frac{1}{3}p_{1R}^2$	Bright rogue wave
	$\frac{1}{3}p_{1R}^2 < (p_{1I} - k_\ell)^2 \leq 3p_{1R}^2$	Intermediate rogue wave
	$(p_{1I} - k_\ell)^2 > 3p_{1R}^2$	Dark rogue wave
$\mathrm{Im}\{f(p_1)\} \neq 0$ or $\mathrm{Im}\{\frac{\partial f(p_1)}{\partial p_1}\} \neq 0$	$0 < (p_{1I} - k_\ell)^2 \leq \frac{1}{3}p_{1R}^2$	Bright lump
	$\frac{1}{3}p_{1R}^2 < (p_{1I} - k_\ell)^2 \leq 3p_{1R}^2$	Bimodel lump
	$(p_{1I} - k_\ell)^2 > 3p_{1R}^2$	Dark lump

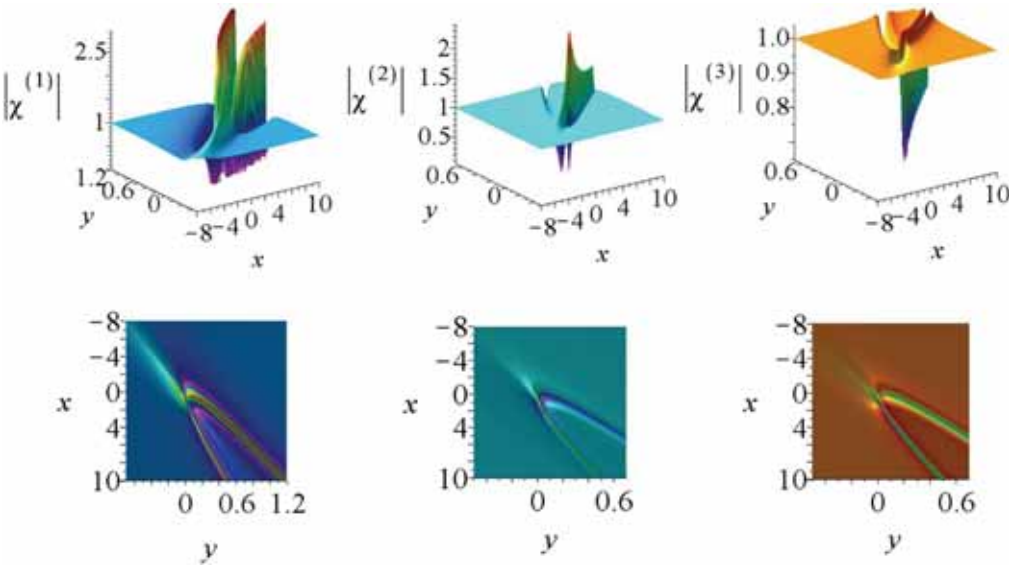

Figure 5. Second-order rogue wave for the multicomponent Mel'nikov system with the same parameters as in figure 4.

Table 3. The classification of fundamental rogue wave solution of the multicomponent Schrödinger–Boussinesq equation.

Region	Types
$0 < (p_{1I} - k_1)^2 \leq \frac{1}{3}p_{1R}^2$	Bright rogue wave
$\frac{1}{3}p_{1R}^2 < (p_{1I} - k_1)^2 \leq 3p_{1R}^2$	Four-petaled rogue wave
$(p_{1I} - k_1)^2 > 3p_{1R}^2$	Dark rogue wave

in Theorem 2, eq. (46) is identified as multirogue wave solutions. Besides, by imposing the parameter constraints

$$\left\{\frac{\mathrm{d}^k f(p_1)}{\mathrm{d}p_1^2} = 0 | k = 0, 1, \ldots, n_i\right\}$$

in Theorem 2, higher-order rogue wave solution can be obtained. For illustrative purpose, the plots of second- and third-order rogue waves for short-wave components are presented in figures 7 and 8. As can be seen in figure 7, second-order rogue wave solutions possess bright–bright, four-petaled–four-petaled and dark–dark rogue waves. Figure 8 depicts third-order rogue waves for the short-wave components, which consist of three fundamental rogue waves in different states.

5. Summary and discussion

In this paper, we obtain exact rational solutions for the multicomponent Mel'nikov system and Schrödinger–Boussinesq equation by employing the Hirota's bilinear method. These solutions are given in terms of determinants. In the multicomponent Mel'nikov system, the fundamental rational solutions possess two different behaviours: lump and line rogue wave. The fundamental lumps have three patterns: bright, bimodel and dark lump. Rogue waves are obtained under particular parameter constraints from general rational solution.

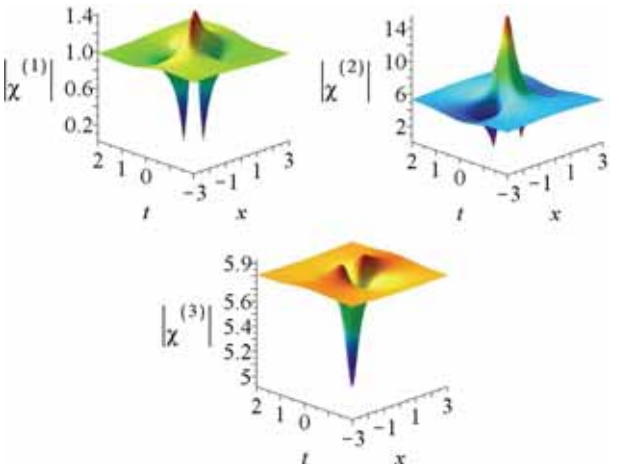

Figure 6. One-rogue wave for the multicomponent Schrödinger–Boussinesq equation with parameters $(\delta_1, \delta_2, \delta_3) = (1, -1, -1)$, $p_1 = 1$, $(k_1, k_2, k_3) = (1, 0, 5)$, $(\rho_1, \rho_2, \rho_3) = (1, 2\sqrt{170}/5, 13\sqrt{5}/5)$.

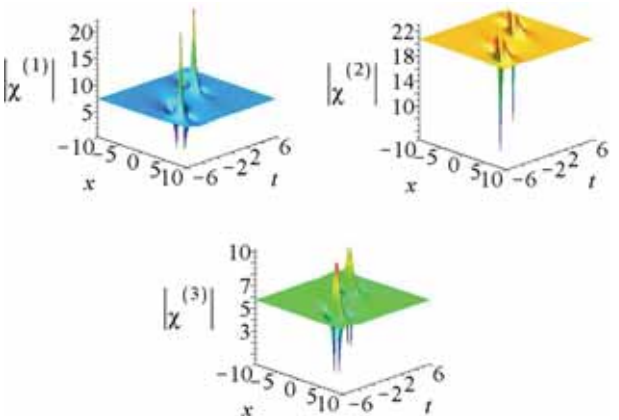

Figure 7. Two-rogue wave for the multicomponent Schrödinger–Boussinesq equation with parameters $(\delta_1, \delta_2, \delta_3) = (1, 1, -1)$, $p_1 = 1+i$, $(k_1, k_2, k_3) = (1, -1, \frac{35-\sqrt{793}}{24})$, $(\rho_1, \rho_2, \rho_3) = (\frac{\sqrt{25109-497\sqrt{793}}}{14}, \frac{5\sqrt{24325-385\sqrt{793}}}{28}, \frac{\sqrt{-1788556+718\sqrt{793}}}{84})$.

Rogue wave behaviours were also classified into three patterns: bright, intermediate and dark rogue waves. We show that the fundamental (simplest) line rogue waves are line rogue waves, which arise from the constant background with a line profile and then disappear into the constant background again. Two subclasses of non-fundamental rogue waves, multi- and higher-order ones, are discussed in detail. The multirogue waves describe the interaction of several fundamental line rogue waves, which generate interesting wave patterns, and the two-rogue waves possess six patterns. The higher-order rogue waves exhibit quiet different dynamic behaviours:

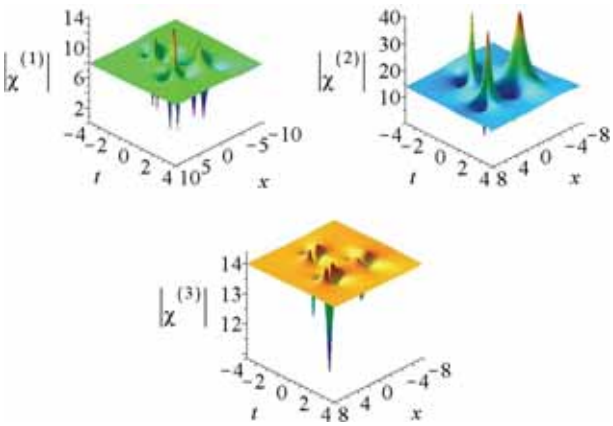

Figure 8. Three-rogue wave for the multicomponent Schrödinger–Boussinesq equation with parameters $(\delta_1, \delta_2, \delta_3) = (-1, -1, -1)$, $p_1 = 1$, $(k_1, k_2, k_3) = (0, \frac{-34+2\sqrt{881}}{4}, \frac{\sqrt{-34+2\sqrt{881}}}{4})$, $(\rho_1, \rho_2, \rho_3) = (\frac{36741+1517\sqrt{881}}{37}, \frac{2709658+50838\sqrt{881}}{148}, \frac{36741+1517\sqrt{881}}{37})$.

wave structure starts from a lump and then retreats back to it, and this transient wave possesses patterns such as parabolas. The second-order rogue waves have three different states.

Further, by considering further reduction, high-order rogue wave solutions of the multicomponent Schrödinger–Boussinesq equation are generated. The fundamental rogue waves can also be classified into three different types: bright, dark and four-petaled rogue waves. Specifically, the dark rogue waves and four-petaled rogue waves have not been reported in the one-component Schrödinger–Boussinesq equation. Dynamical profiles of the non-fundamental rogue waves are also exhibited.

Acknowledgements

This work was supported by the Shandong Provincial Natural Science Foundation (Grant No. ZR2015PD009), the National Natural Science Foundation of China (Grant No. 41506037), and the National Key Research and Development Programme of China (Grant Nos 2016YFC1402000, 2016YFC1402304).

References

[1] K Dysthe, H E Krogstad and P Müller, *Annu. Rev. Fluid Mech.* **40**, 287 (2008)

[2] D R Solli, C Ropers, P Koonath and B Jalali, *Nature* **450**, 1054 (2007)

[3] B Kibler, J Fatome, C Finot, G Millot, F Dias, F Genty, N Akhmediev and J M Dudley, *Nat. Phys.* **6**, 790 (2010)
[4] Y V Bludov, V V Konotop and N Akhmediev, *Phys. Rev. A* **80**, 033610 (2009)
[5] H Bailung, S K Sharma and Y Nakamura, *Phys. Rev. Lett.* **107**, 255005 (2011)
[6] M Shats, H Punzmann and H Xia, *Phys. Rev. Lett*. **104**, 104503 (2010)
[7] M Onorato, S Residori, U Bortolozzo, A Montina and F T Arecchi, *Phys. Rep.* **528**, 47 (2013)
[8] A Chabchoub, N P Hoffmann and N Akhmediev, *Phys. Rev. Lett.* **106**, 204502 (2011)
[9] A Chabchoub, N Hoffmann, M Onorato and N Akhmediev, *Phys. Rev. X* **2**, 011015 (2012)
[10] N N Akhmediev and V I Korneev, *Theor. Math. Phys.* **69**, 1089 (1986)
[11] V E Zakharov and A I Dyachenko, *Eur. J. Mech. B* **29**, 127 (2010)
[12] N Akhmediev, J M Soto-Crespo and A Ankiewicz, *Phys. Rev. A* **80**, 043818 (2009)
[13] V E Zakharov and L A Ostrovsky, *Physica D* **238**, 540 (2009)
[14] D H Peregrine, *J. Aust. Math. Soc. B* **25**, 16 (1983)
[15] N Akhmediev, A Ankiewicz and M Taki, *Phys. Lett. A* **373**, 675 (2009)
[16] Z X Xu and K W Chow, *Appl. Math. Lett*. **56**, 72 (2016)
[17] Y Ohta and J Yang, *Proc. R. Soc. London Ser. A* **468**, 1716 (2012)
[18] Y S Tao and J S He, *Phys. Rev. E* **85**, 026601 (2012)
[19] G Mu, Z Y Qin and R Grimshaw, *SIAM J. Appl. Math.* **75**, 1 (2015)
[20] J S He, H R Zhang, L H Wang, K Porsezian and A S Fokas, *Phys. Rev. E* **87**, 052914 (2013)
[21] L H Wang, K Porsezian and J S He, *Phys. Rev. E* **87**, 053202 (2013)
[22] Z Y Yan, V V Konotop and N Akhmediev, *Phys. Rev. E* **82**, 036610 (2010)
[23] S Chen and D Mihalache, *J. Phys. A: Math. Theor.* **48**, 215202 (2015)
[24] X Wang, Y Q Li, F Huang and Y Chen, *Commun. Nonlinear Sci. Numer. Simul.* **20**, 434 (2015)
[25] S H Chen, J M Soto-Crespo, F Baronio, P Grelu and D Mihalache, *Opt. Express* **24**, 15251 (2016)
[26] F Baronio, S Wabnitz and Y Kodama, *Phys. Rev. Lett.* **116**, 173901 (2016)
[27] J G Rao, K Porsezian and J S He, *Chaos* **27**, 083115 (2017)
[28] A Ankiewicz and N Akhmediev, *Rom. Rep. Phys.* **69**, 104 (2017)
[29] Y B Liu, A S Fokas, D Mihalache and J S He, *Rom. Rep. Phys.* **68**, 1425 (2016)
[30] F Yuan, J G Rao, K Porsezian, D Mihalache and J S He, *Rom. J. Phys.* **61**, 378 (2016)
[31] S H Chen, P Grelu, D Mihalache and F Baronio, *Rom. Rep. Phys.* **68**, 1407 (2016)
[32] H Chen and W W Chen, *Rom. Rep. Phys*. **69**, 3 (2017)
[33] W Liu, *Rom. Rep. Phys*. **62**, 3 (2017)
[34] Y Ohta and J K Yang, *Phys. Rev. E* **86**, 036604 (2012)
[35] Y Ohta and J K Yang, *J. Phys. A: Math. Theor*. **46**, 105202 (2013)
[36] P Dubard and V B Matveev, *Nonlinearity* **26**, 93 (2013)
[37] J G Rao, L H Wang, Y Zhang and J S He, *Commun. Theor. Phys.* **64**, 605 (2015)
[38] Y K Liu and B Li, *Pramana – J. Phys*. **88**, 57 (2017)
[39] H Gao, *Pramana – J. Phys.* **88**, 84 (2017)
[40] N Vishnu, M Senthilvelan and M Lakshmana, *Pramana – J. Phys.* **84**, 339 (2015)
[41] W Chen, H L Chen and Z D Dai, *Pramana – J. Phys*. **86**, 713 (2016)
[42] D Mihalache, *Rom. Rep. Phys*. **67**, 1383 (2015)
[43] D Mihalache, *Rom. Rep. Phys*. **69**, 403 (2017)
[44] F Baronio, A Degasperis, M Conforti and S Wabnitz, *Phys. Rev. Lett.* **109**, 044102 (2012)
[45] N Yajima and M Oikawa, *Prog. Theor. Phys*. **56**, 1719 (1976)
[46] Y Ohta, K Maruno and M Oikawa, *J. Phys. A: Math. Gen*. **40**, 7659 (2017)
[47] Z Han, Y Chen and J C Chen, *J. Phys. Soc. Jpn.* **86**, 074005 (2017)
[48] A Hasegawa and Y Kodama, *Solitons in optical communications* (Clarendon, Oxford, 1995)
[49] A C Scott, *Nonlinear science: Emergence and dynamics of coherent structures* (Oxford University Press, Oxford, 1999)
[50] G P Agrawal, *Nonlinear fiber optics* (Academic Press, New York, 1995)
[51] Y S Kivshar and G P Agrawal, *Optical solitons: From fibers to photonic crystals* (Academic Press, San Diego, 2003)
[52] L Q Kong and C Q Dai, *Nonlinear Dyn.* **81**, 1553 (2015)
[53] B L Guo and L M Ling, *Chin. Phys. Lett.* **28**, 110202 (2011)
[54] Y V Bludov, V V Konotop and N Akhmediev, *Eur. Phys. J. Spec. Top.* **185**, 169 (2010)
[55] Z Han and Y Chen, *Bright–dark mixed N-soliton solutions of the multicomponent Mel'nikov system*, arXiv:1706.06881
[56] V K Mel'nikov, *Lett. Math. Phys.* **7**, 129 (1983)
[57] V K Mel'nikov, *Phys. Lett. A* **118**, 22 (1986)
[58] V K Mel'nikov, *J. Math. Phys.* **28**, 2603 (1987)
[59] V K Mel'nikov, *Commum. Math. Phys.* **112**, 639 (1987)
[60] Y Hase, R Hirota and Y Ohta, *J. Phys. Soc. Jpn.* **58**, 2713 (1989)
[61] C Senthil Kumar, R Radha and M Lakshmanan, *Chaos Solitons Fractals* **22**, 705 (2004)
[62] G Mu and Z Y Qin, *Nonlinear Anal. Real World Appl.* **18**, 1 (2014)
[63] S V Singh, N N Rao and P K Shukla, *J. Plasma Phys.* **60**, 551 (1998)
[64] Y Hase and J Satsuma, *J. Phys. Soc. Jpn.* **57**, 679 (1988)
[65] A R Chowdhury, B Dasgupta and N N Rao, *Chaos Solitons Fractals* **9**, 1747 (1998)
[66] X B Hu, B L Guo and H E Tam, *J. Phys. Soc. Jpn.* **72**, 189 (2003)
[67] G Mu and Z Y Qin, *J. Phys. Soc. Jpn.* **81**, 084001 (2012)

[68] M Jimbo and T Miwa, *Publ. RIMS Kyoto Univ.* **19**, 943 (1983)
[69] Y Ohta, D Wang and J Yang, *Stud. Appl. Math*. **127**, 345 (2011)
[70] R Hirota, *The direct method in soliton theory* (Cambridge University Press, Cambridge, UK, 2004)
[71] J C Chen, Y Chen, B F Feng and K Maruno, *Phys. Lett. A* **379**, 1510 (2015)
[72] Y K Shi, Line rogue waves in the Mel'nikov equation (accepted by *Z. Naturforsch A* 2017)
[73] J Rao, Y Cheng and J S He, *Stud. Appl. Math.* **139**, 568 (2017)